ChemComm

Accepted Manuscript

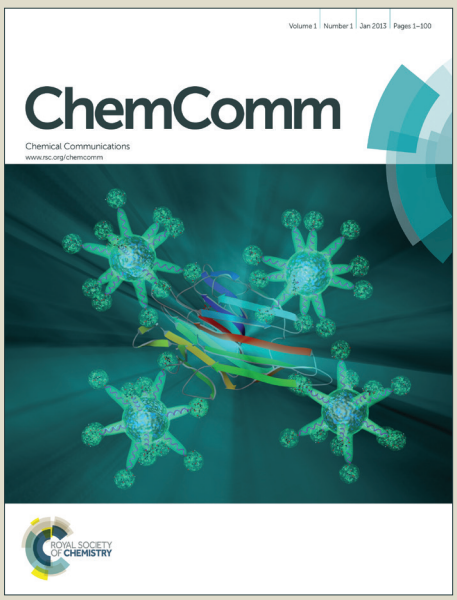

ROYAL SOCIETY OF CHEMISTRY

www.rsc.org/chemcomm

ARTICLE TYPE www. rsc.org/xxxxxx | XXXXXXXX

Water Adsorption in UiO-66: The Importance of Defects†

Pritha Ghosh, Yamil J. Colón, and Randall Q. Snurr*

Received Xth XXXXXXXXXX 20XX, Accepted Xth XXXXXXXXX 20XX
First published on the web Xth XXXXXXXXXX 200X
DOI: 10.1039/b000000x

Simulated adsorption isotherms for water in UiO-66 illustrate that defects in the form of missing linkers make this MOF more hydrophilic. Heats of adsorption and density plots further confirm the effect of defects on adsorption of water in UiO-66 at low loadings. In addition, water and CO_2 isotherms indicate that not only the amount of defects but their locations within the material affect the loading of guest molecules.

Metal-organic frameworks (MOFs) are porous crystalline materials made up of inorganic nodes connected by organic linkers. Due to their porosity and their chemically tunable nature, MOFs are being assessed for use in a variety of adsorption applications; however, many MOFs are unstable in the presence of water, thereby drastically limiting their usefulness.[1–3] UiO-66 is a MOF whose inorganic node is a $Zr_6O_4(OH)_4$ cluster, a common motif in MOFs able to withstand water and high temperature.[4,5] Most water-stable MOFs are hydrophobic, and exhibit Type V[6] isotherms.[7] While there is no generally accepted definition of hydrophobicity in porous materials, the pressure at which the pores fill with water is a convenient metric.[8] Highly hydrophobic MOFs, such as ZIF-8, do not show appreciable uptake of water until near the saturation vapor pressure of water, while hydrophilic MOFs adsorb water at very low pressures.[9] Experimental water isotherms for UiO-66 show water condensation in the pores at 30% relative humidity,[10–12] which is unusually low for a water-stable MOF.

In this work, we used grand canonical Monte Carlo simulations to study the adsorption of water in hydroxylated UiO-66, following the methodology we used previously for a set of hydrophobic MOFs.[8] Lennard-Jones parameters for the framework were taken from the DREIDING[13] force field, except for zirconium, which was taken from UFF.[14] Framework charges were calculated with the REPEAT[15] method. The TIP4P[16] model was used for water, and the TraPPE[17] model was used for CO_2. Experimental results in the literature[5,18,19] have shown that UiO-66 samples often contain defects in the form of missing linkers. To model this, we created two defect unit cells in which each Zr node is missing one linker (out of 12 total), and each missing linker is replaced by 4 hydroxyl groups (2 on each node it was connected to). While the number of defects present in each defect unit cell is identical, the location of these defects differs between the two unit cells.

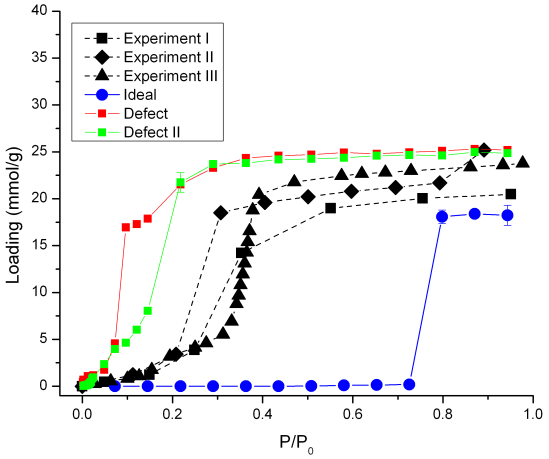

Fig. 1 Water isotherms for UiO-66 at 298 K from simulation (ideal unit cell and two defect unit cells) and experiments I[10], II[11], and III[12]

Figure 1 compares experimental[10–12] water isotherms to simulation results for the ideal unit cell and the two defect unit cells. The ideal unit cell isotherm predicts water condensation around 0.7 P/P_0, and a lower saturation loading than any of the experimental results. On the other hand, the unit cells with defects show water condensation in the pores around 0.1 and 0.2 P/P_0, along with a higher saturation loading than the experimental results. The shape of the isotherms for the defect unit cells is a closer fit to the experimental results, showing a more gradual ascent. Even the slight shoulder visible in Experiment I can be seen in the first defect unit cell. The saturation loadings suggest that there are fewer linkers missing in the experimental samples than in our defect-laden unit cells.

† Electronic Supplementary Information (ESI) available: All simulation details including structure files with partial charges, pore size distributions for each structure, details of BET calculations including N_2 isotherms, and heats of adsorption for CO_2. See DOI: 10.1039/b000000x/

Department of Chemical & Biological Engineering, Northwestern University, 2145 Sheridan Road, Evanston, Illinois 60208, USA. E-mail: snurr@northwestern.edu; Tel: +1-847-467-2977

Adsorption of water in these materials is affected by both the number of defects and their location.

In order to better characterize the presence of defects in the experimental materials, we examined the nitrogen isotherms. Experiment I[10] does not report N_2 isotherms for their sample. Experiment II[11] reports a BET surface area of 1160 m^2/g, and their nitrogen isotherm[20] shows a saturation loading of around 350 cm^3/g at $P/P_0 = 0.8$. Experiment III[12] reports a BET surface area of 1290 m^2/g and a saturation loading of 320 cm^3/g. From simulated nitrogen isotherms, we calculate a BET surface area of 1280 m^2/g and a nitrogen saturation loading of around 300 cm^3/g for the ideal unit cell. For the first defect unit cell, we calculate a BET surface area of 1400 m^2/g and a saturation loading of around 330 cm^3/g. The experimental BET surface areas are close to our ideal BET surface area; however, the experimental nitrogen saturation loadings are both greater than that predicted for our ideal unit cell. These values, along with Figure 1, illustrate how a small number of defects (which lead to only small differences in the BET surface area and the nitrogen saturation loading) can have a profound effect on the adsorption of water in UiO-66.

In addition to running water adsorption isotherms, we also ran the desorption isotherm in the ideal unit cell and observed large hysteresis (see Supporting Information), with water exiting the pores around 0.25 P/P_0 as shown in Figure S5. Hysteresis in GCMC simulations is strongly related to the mechanisms in experimental hysteresis, with the exception of any pore blockage effects (which are unlikely in this scenario).[21] Hysteresis can be found in the water isotherms (both experimental and simulation) of many hydrophobic MOFs,[7,22–24] though it is notable that ZIF-8 does not exhibit any hysteresis.[9] For UiO-66, only Experiment III[12] reports a desorption isotherm, which shows slight hysteresis (see Figure S5).

The difference in hydrophobicity between the ideal and defective unit cells is further clarified by the heats of adsorption, Q_{st}, as seen in Figure 2. The heats of adsorption for the ideal unit cell follow the same shape as seen previously for other hydrophobic MOFs,[8] with values around 15 kJ/mol at low loading and then rising sharply and plateauing at 60 kJ/mol. In contrast, the heats of adsorption calculated for the unit cells with defects show a Q_{st} at low loading around 70 kJ/mol or 60 kJ/mol, which then gradually decreases to around 55 kJ/mol at saturation loading. This curve looks very similar to those reported for MOFs with functional groups, where high Q_{st} values at low loadings are standard, due to strong adsorption at the functional groups. This suggests that the defects in UiO-66 cause it to be more hydrophilic.

Density distributions of water in both the ideal and the first defective unit cell at low loadings further corroborate the importance of these defect sites, as shown in Figure 3. At $P/P_0 = 0.07$ (300 Pa) the defect isotherm has a higher loading than its ideal counterpart. However, the density plot of the defect

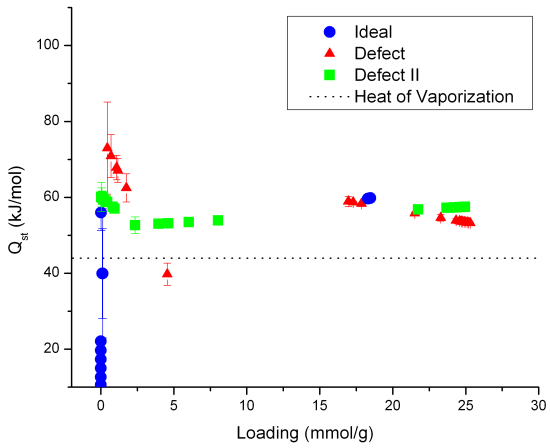

Fig. 2 Simulated heats of adsorption for water in an ideal unit cell of UiO-66 and two defect unit cells at 298 K

unit cell shows concentrated adsorption sites between the two hydroxyls left by each missing linker on a Zr node. In contrast, the ideal unit cell shows more diffuse density clouds, especially given that it has a lower uptake than the defective one. In fact, the loading in the first small plateau of the defect isotherm, at 0.024 P/P_0, is 58 molecules per 128 hydroxyl groups, which corresponds to roughly one water molecule between every pair of hydroxyl groups.

If a small number of defects can have such significant effects on water adsorption, they may also affect the adsorption of other small molecules. Figure 4 shows simulated CO_2 isotherms for the ideal and defect unit cells compared with experiment. Not only is there a large difference between the isotherms for the ideal and defect unit cells, there is a significant difference in the isotherms for the two defect unit cells. As noted above, it is not only the amount of defects but also the location of those defects that can have a significant effect on adsorption. The heats of adsorption for CO_2 in UiO-66 can be found in Figure S6, and both of the defective unit cells show high heats of adsorption at low loadings. Experiments I and V also follow this trend; however Experiment IV shows a gradual increase in the heats of adsorption as the loading increases.

In conclusion, the ideal UiO-66 unit cell shows hydrophobic behavior, as quantified by water condensing in the pores at around 80% relative humidity. Missing organic linkers in UiO-66 create defect sites which make the MOF more hydrophilic, although experimentally, other defects in the crystals and impurities may also affect the observed behavior. The location of defects can lead to significant differences in adsorption, as shown by simulated water and CO_2 isotherms. These findings are similar to what has been observed for

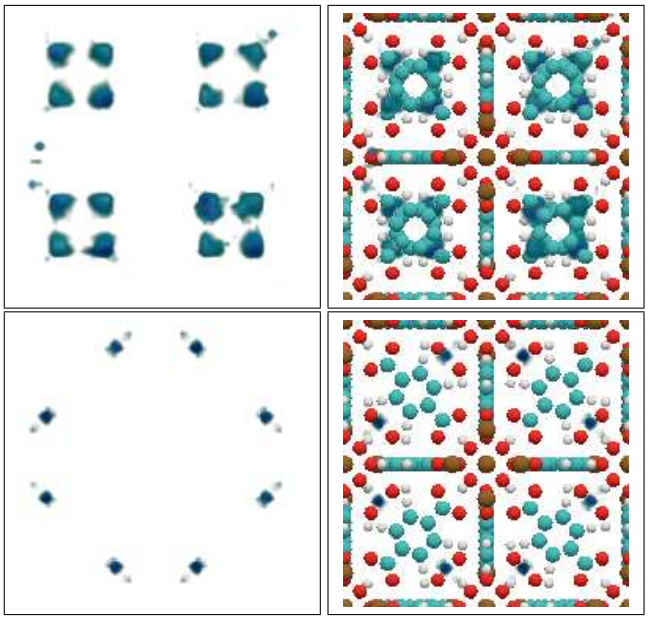

Fig. 3 Density distributions of water in UiO-66: ideal (top) and defective (bottom) unit cells at 300 Pa and 298 K; lefthand column, without framework atoms; righthand column, with framework atoms overlaid

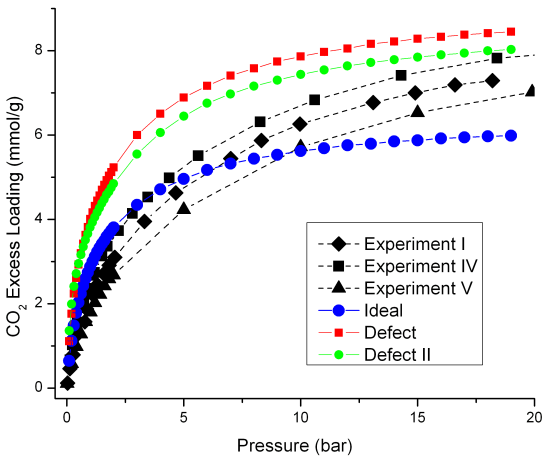

Fig. 4 CO_2 adsorption isotherms at 300 K from simulation (ideal and two defect unit cells) and experiments I[10], IV[19], and V[20]

silanol defects in silicalite,[25] where the number and the relative location of the silanols is crucial to the formation of water clusters. This work also supports the idea of Thommes et al.[26,27] that water isotherms can be used to characterize porous materials in combination with nitrogen and argon adsorption. In UiO-66, experimental BET surface areas and nitrogen saturation loadings do not definitively suggest any deviation from the ideal unit cell, but the water isotherms are quite sensitive to the presence of defects.

Acknowledgements

This work was supported by the Defense Threat Reduction Agency (HDTRA1-10-1-0023) and by a National Science Foundation Graduate Research Fellowship to YJC (Grant No. DGE-0824162).

References

1 J. J. Low, A. I. Benin, P. Jakubczak, J. F. Abrahamian, S. A. Faheem and R. R. Willis, *Journal of the American Chemical Society*, 2009, **131**, 15834–42.
2 K. A. Cychosz and A. J. Matzger, *Langmuir*, 2010, **26**, 17198–202.
3 J. Liu, A. I. Benin, A. M. B. Furtado, P. Jakubczak, R. R. Willis and M. D. LeVan, *Langmuir*, 2011, **27**, 11451–6.
4 J. H. Cavka, S. Jakobsen, U. Olsbye, N. Guillou, C. Lamberti, S. Bordiga and K. P. Lillerud, *Journal of the American Chemical Society*, 2008, **130**, 13850–1.
5 L. Valenzano, B. Civalleri, S. Chavan, S. Bordiga, M. H. Nilsen, S. Jakobsen, K. P. Lillerud and C. Lamberti, *Chemistry of Materials*, 2011, **23**, 1700–1718.
6 K. S. W. Sing, D. H. Everett, R. A. W. Haul, L. Moscou, R. A. Pierotti, J. Rouquerol and T. Siemieniewska, *Pure and Applied Chemistry*, 1985, **57**, 603–619.
7 J. Canivet, A. Fateeva, Y. Guo, B. Coasne and D. Farrusseng, *Chemical Society Reviews*, in press. DOI: 10.1039/c4cs00078a.
8 P. Ghosh, K. C. Kim and R. Q. Snurr, *The Journal of Physical Chemistry C*, 2014, **118**, 1102–1110.
9 P. Küsgens, M. Rose, I. Senkovska, H. Fröde, A. Henschel, S. Siegle and S. Kaskel, *Microporous and Mesoporous Materials*, 2009, **120**, 325–330.
10 A. D. Wiersum, E. Soubeyrand-Lenoir, Q. Yang, B. Moulin, V. Guillerm, M. B. Yahia, S. Bourrelly, A. Vimont, S. Miller, C. Vagner, M. Daturi, G. Clet, C. Serre, G. Maurin and P. L. Llewellyn, *Chemistry, an Asian Journal*, 2011, **6**, 3270–80.
11 P. M. Schoenecker, C. G. Carson, H. Jasuja, C. J. J. Flemming and K. S. Walton, *Industrial & Engineering Chemistry Research*, 2012, **51**, 6513–6519.
12 H. Furukawa, F. Gándara, Y.-B. Zhang, J. Jiang, W. L. Queen, M. R. Hudson and O. M. Yaghi, *Journal of the American Chemical Society*, 2014, **136**, 4369–81.
13 S. L. Mayo, B. D. Olafson and W. A. Goddard III, *Journal of Physical Chemistry*, 1990, **94**, 8897–8909.
14 A. K. Rappe, C. J. Casewit, K. S. Colwell, W. A. Goddard III and W. M. Skiff, *Journal of the American Chemical Society*, 1992, **114**, 10024–10035.
15 C. Campañá, B. Mussard and T. K. Woo, *Journal of Chemical Theory and Computation*, 2009, **5**, 2866–2878.
16 W. L. Jorgensen, J. Chandrasekhar, J. D. Madura, R. W. Impey and M. L. Klein, *The Journal of Chemical Physics*, 1983, **79**, 926–935.
17 J. J. Potoff and J. I. Siepmann, *AIChE Journal*, 2001, **47**, 1676–1682.
18 M. J. Katz, Z. J. Brown, Y. J. Colón, P. W. Siu, K. A. Scheidt, R. Q. Snurr, J. T. Hupp and O. K. Farha, *Chemical Communications*, 2013, **49**, 9449–51.
19 H. Wu, Y. S. Chua, V. Krungleviciute, M. Tyagi, P. Chen, T. Yildirim and W. Zhou, *Journal of the American Chemical Society*, 2013, **135**, 10525–32.
20 G. E. Cmarik, M. Kim, S. M. Cohen and K. S. Walton, *Langmuir*, 2012,

28, 15606–13.
21 L. Sarkisov and P. A. Monson, *Langmuir*, 2000, **16**, 9857–9860.
22 N. M. Padial, E. Quartapelle Procopio, C. Montoro, E. López, J. E. Oltra, V. Colombo, A. Maspero, N. Masciocchi, S. Galli, I. Senkovska, S. Kaskel, E. Barea and J. A. R. Navarro, *Angewandte Chemie (International ed. in English)*, 2013, **52**, 8290–4.
23 A. Nalaparaju and J. Jiang, *Langmuir*, 2012, **28**, 15305–12.
24 A. Comotti, S. Bracco, P. Sozzani, S. Horike, R. Matsuda, J. Chen, M. Takata, Y. Kubota and S. Kitagawa, *Journal of the American Chemical Society*, 2008, **130**, 13664–72.
25 A. O. Yazaydin and R. W. Thompson, *Microporous and Mesoporous Materials*, 2009, **123**, 169–176.
26 M. Thommes, S. Mitchell and J. Pérez-Ramírez, *The Journal of Physical Chemistry C*, 2012, **116**, 18816–18823.
27 M. Thommes, J. Morell, K. A. Cychosz and M. Fröba, *Langmuir*, 2013, **29**, 14893–902.